Proceedings of *RAGtime 10–13, 15–17/20–22/15–17/14–16 September, 2008/2009/2010/2011, Opava, Czech Republic*
Z. Stuchlík, G. Török and T. Pecháček, editors, Silesian University in Opava, 2014, pp. 37–44

Critical curves of triple gravitational microlenses

Kamil Daněk and David Heyrovský

Institute of Theoretical Physics, Faculty of Mathematics and Physics,
Charles University, Prague, Czech Republic

ABSTRACT
In the theory of gravitational lensing the lens caustic and its primary image, the critical curve, have fundamental importance. Knowledge of these curves greatly facilitates the interpretation and analysis of time-dependent gravitational microlensing events. A binary lens modelled by two point masses can form caustics of three different topologies, which correspond to three topologies of the critical curve. Here we analyse critical curve topologies of the triple lens. While the binary lens is characterized by two parameters, five parameters are needed to describe the triple lens. We present an example illustrating the analysis of special triple-lens models described by two parameters. We find analytical conditions for the change of critical-curve topology, which define boundaries of regions in parameter space with different critical-curve topology. For each region we present corresponding critical curves and caustics. We also include sample results for a three-parameter model describing a triple lens with equal masses in a general spatial configuration.

1 INTRODUCTION

Gravitational microlensing is a special regime of gravitational lensing in which the lensing body is of stellar or sub-stellar mass, so that the deflection angle is too small for resolving individual images of a background star (the "source" in lensing terminology). The main measurable quantity is the time-dependent amplification of flux from the source, i.e. the light curve of a microlensing event. The amplification peaks sharply when the source crosses the caustic of the lens, which – if we could resolve individual images – corresponds to the formation or destruction of a pair of images on the critical curve of the lens.

The single-point-mass lens was discussed in detail by Refsdal (1964). The first theoretical study of two-point-mass lenses was carried out by Schneider and Weiss (1986) who described the properties of the critical curve and caustic of an equal-mass binary lens. A complete analysis of caustic and critical-curve topologies of the general binary lens was performed by Erdl and Schneider (1993).

The first convincing triple-lens microlensing event, OGLE-2006-BLG-109, was found in 2006 (Gaudi et al. 2008). The lens system consisted of a star with two planets forming a Sun + Jupiter + Saturn analogue. The possibility of detecting triple lenses was discussed in several papers (e.g. star with an exoplanet with a moon by Liebig and Wambsganss 2010, Han 2008; planet in a binary-star system by Lee et al. 2008, Chung and Park 2010).

978-80-7510-125-9

At the same time, gravitational microlensing by a system of three bodies has not been satisfactorily analysed theoretically yet. Inspired by the Erdl and Schneider (1993) analysis of the parameter dependence of binary lensing, we extend their approach to special cases of the triple lens, focusing here on the classification of critical-curve topologies.

For binary lenses, there are only three different topologies of the critical curve, corresponding to three different topologies of the caustic. These are usually labelled according to the binary separation as "close" (critical curve formed by three loops), "resonant" (one loop), and "wide" (two loops), with boundaries between the regimes depending on the binary mass ratio. Apart from the merger of loops at these boundaries, the loops of a binary lens caustic never self-intersect, never intersect mutually, and are never nested. The more complex triple-lens caustics often exhibit self-intersections, loop intersections and loop nesting without a change in critical-curve topology. However, the number of loops of the caustic is always the same as the number of loops of the critical curve. In the following we classify the critical-curve topologies by studying the conditions for the merger of critical-curve loops. Such a classification may then serve as a basis for classifying the topologies of the triple-lens caustic.

2 CRITICAL CURVES IN GRAVITATIONAL MICROLENSING

For an n-point-mass lens system, the equation tying the position of the source and its images may be expressed in complex form as

$$\zeta = z - \sum_{i=1}^{n} \frac{\mu_i}{\bar{z} - \bar{z}_i}\,, \tag{1}$$

where ζ is the source position, z is the image position in the lens plane, z_i are the point-mass positions (barred variables $\bar{z}$, $\bar{z_i}$ are complex conjugates of z, z_i), and μ_i are their relative masses with unit total mass ($\sum_{i=1}^{n} \mu_i = 1$). This complex notation was introduced by Witt (1990). All angular positions are normalized to the total-mass Einstein radius, i.e. the radius of a ring-shaped image of a source positioned directly behind a single lens. The amplification of a given image is obtained as the reciprocal value of the determinant of the Jacobi matrix of lens Eq. (1), $J = (\partial\zeta/\partial z)$. The equation of the critical curve is obtained by setting $\det J = 0$, which leads to

$$\sum_{i=1}^{n} \frac{\mu_i}{(z - z_i)^2} = e^{-2\mathrm{i}\phi}\,, \tag{2}$$

where the real phase ϕ varies along the curve from 0 to 2π.

The critical curve in fact is the $\det J = 0$ contour of the Jacobian in the lens plane. Hence, it forms the boundary between regions of positive and negative $\det J$. As a consequence, the point on a critical curve at which loops of the critical curve merge must also be a saddle point of $\det J$. The additional saddle-point condition for such a merging point can be computed from the Hessian, which yields

$$\sum_{i=1}^{n} \frac{\mu_i}{(z - z_i)^3} = 0\,. \tag{3}$$

By solving (2) and (3) simultaneously we get analytic conditions for merging points. These define the boundaries separating regions in parameter space with different critical-curve topologies.

3 TRIPLE LENS: TWO-PARAMETER MODEL

The triple lens is described by five parameters: two relative masses and three position parameters. Finding the merger conditions as equations combining all five parameters is prohibitive because of algebraic complexity and thus demands on computational time. Therefore, we used special triple-lens models with fewer free parameters for an initial exploration of the parameter space.

To give a two-parameter example, we present here the results for a triple-lens system in an equilateral triangle configuration with two masses set equal. Our variable parameters are the mass μ of the third lens, and the length d of a side of the triangle. Using the Sylvester matrix method of Erdl and Schneider (1993), we get four independent conditions for critical-curve merger. Two of them have a similar form, both being polynomials of sixth degree in d^2:

$$a_{12}d^{12} + a_{10}d^{10} + a_8d^8 + a_6d^6 + a_4d^4 + a_2d^2 + a_0 = 0\,, \tag{4}$$
$$a_{12}d^{12} - a_{10}d^{10} + a_8d^8 - a_6d^6 + a_4d^4 - a_2d^2 + a_0 = 0\,, \tag{5}$$

where

$$\begin{aligned}
a_{12} &= 32\,,\\
a_{10} &= 48(3\mu - 1)\,,\\
a_8 &= -48(3\mu - 1)(3\mu - 5)\,,\\
a_6 &= 8\big(81\mu^3 + 27\mu^2 - 45\mu + 35\big)\,,\\
a_4 &= 6(3\mu - 1)\big(621\mu^3 - 981\mu^2 + 351\mu + 25\big)\,,\\
a_2 &= -3(3\mu - 1)\big(243\mu^4 - 972\mu^3 + 1098\mu^2 - 372\mu - 13\big)\,,\\
a_0 &= -108\mu^3 + 324\mu^2 - 180\mu - 4\,.
\end{aligned} \tag{6}$$

The third has the form of a polynomial of third degree in d^4,

$$\begin{aligned}
&16d^{12} - 24\big(9\mu^2 - 6\mu - 1\big)d^8 - \big(243\mu^4 + 972\mu^3 + 1134\mu^2 - 468\mu + 15\big)d^4 +\\
&+54\mu^3 - 162\mu^2 + 90\mu + 2 = 0\,,
\end{aligned} \tag{7}$$

and the fourth is a polynomial of twelfth degree in d^4,

$$\sum_{l=0}^{12} b_{4l}d^{4l} = 0\,, \tag{8}$$

where b_{4l} are functions of μ that we don't specify here due to their complexity.

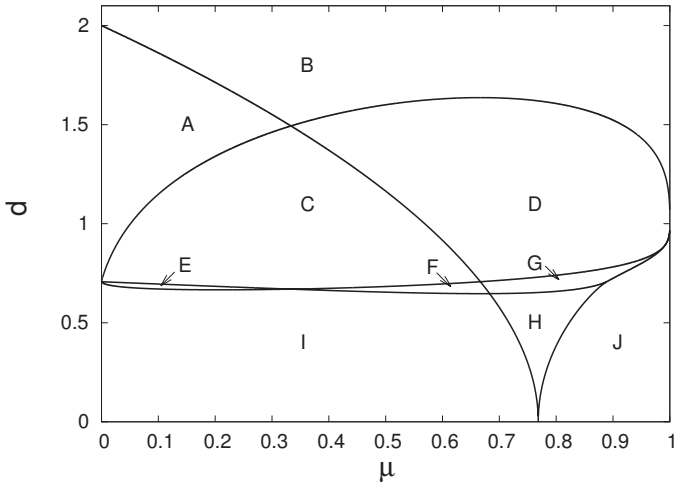

Figure 1. Parameter space regions according to critical-curve topology for a triple lens in an equilateral triangle configuration. Parameters: mass of vertex μ; length of side d.

The curves in the $[\mu, d]$ plane given implicitly by Eqs. (4), (5), (7), and (8) form boundaries that divide the parameter space into several regions. To make sure that regions on either side of each curve correspond to different topologies, it is necessary to check whether each solution of (4), (5), (7), and (8) also fulfils the original conditions (2) and (3).

In Figure 1 we plotted the parameter space of the equilateral-triangle lens with curves given by (4), (5), (7), and (8). These curves divide the parameter space into ten regions, labelled in the Figure A through J. Examples of critical curves and caustics from all ten regions are shown in Fig. 2. There are altogether seven different topologies of the critical curve. The topologies in E and G are the same, so are those in F and H, and in I and J. The critical curve in B consists of three loops that separate in the limit $d \to \infty$ into Einstein rings of three single lenses. The critical curve in I and J consists of an outer loop and four inner loops. In the limiting case $d \to 0$ the inner loops disappear at the lens position and the outer loop turns into the Einstein ring of a single lens with total mass $\sum_{i=1}^{3} \mu_i = 1$.

The analysis of two other two-parameter models can be found in Daněk (2010).

4 TRIPLE LENS: THREE-PARAMETER MODEL

Using the Sylvester matrix method for three-parameter triple-lens configurations usually leads to multi-page expressions for merging conditions. Factorizing the final result into separate surfaces dividing the parameter space presents a further hurdle to this method. It is necessary, therefore, to find an alternative approach.

We noticed a nice property of (2) and (3) that can be used to obtain the parameters of critical-curve mergers. If we multiply both sides of (2) by a real positive number α and perform the transformation $z' = \alpha^{-1/2} z$, $z'_i = \alpha^{-1/2} z_i$, we obtain the equation of

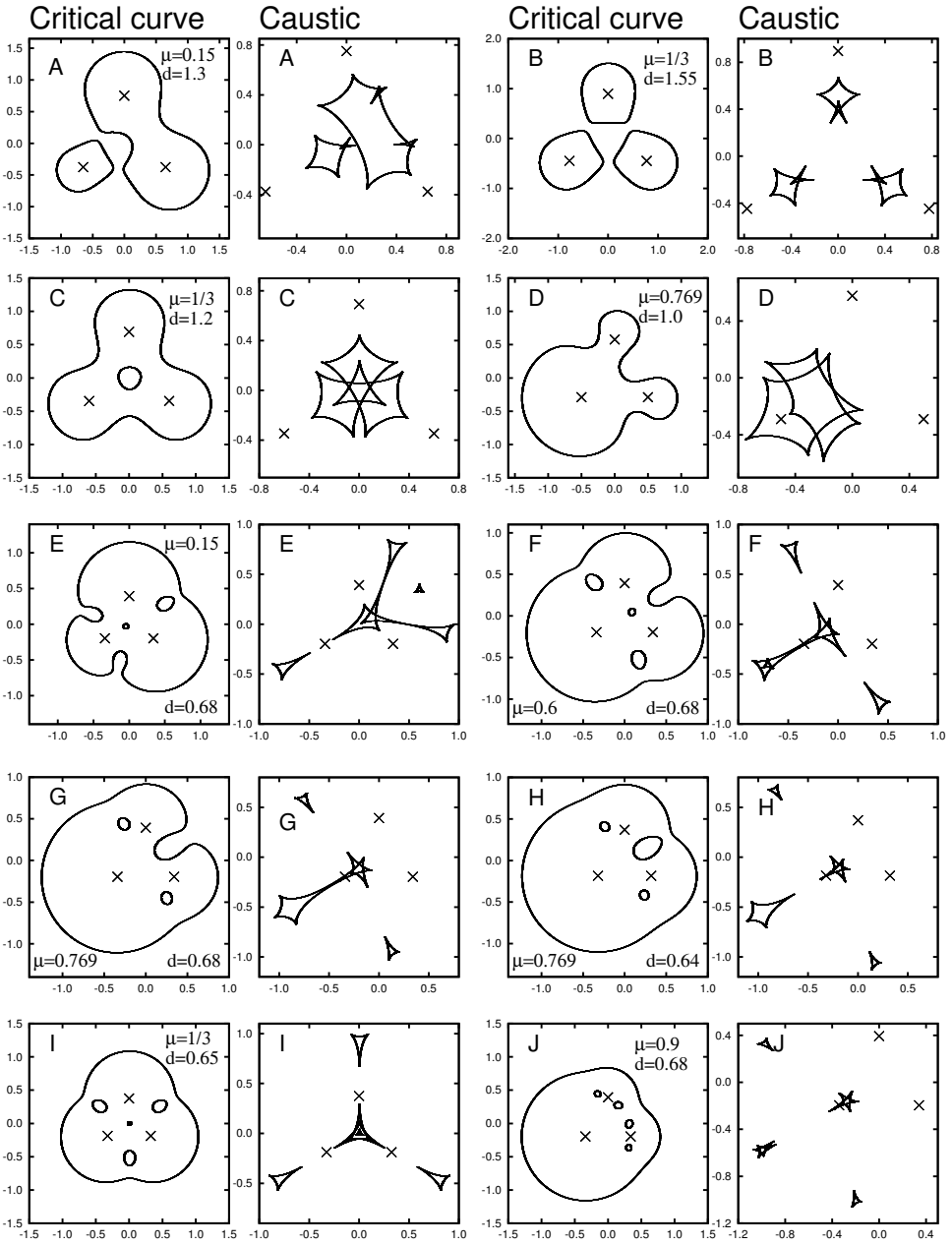

Figure 2. Critical curves and caustics of a triple lens in an equilateral triangle configuration. First and third column: critical curves; second and fourth column: caustics; crosses: lens positions. Letters labelling the panels correspond to regions in Fig. 1.

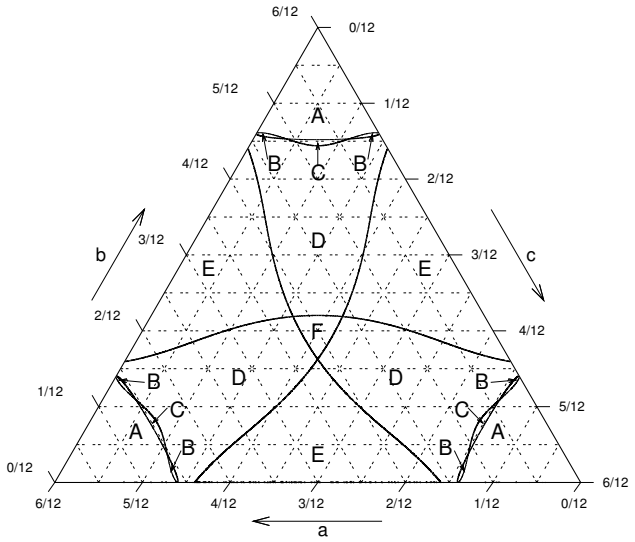

Figure 3. Parameter space regions according to critical-curve topology for a triple lens with equal masses and circumference $o = 4.8$. Lengths of sides a, b, c are in units of o.

a Jacobian contour line with $\det J' = 1 - \alpha^2$ in z'. The saddle-point condition (3) holds for both transformed and untransformed values. This enables us to find the value of $\det J'$ in a saddle point z' for some chosen lens positions ${z'}_i$ and a contour line going through the saddle point. By inverting the transformation we can find lens parameters z_i with a critical curve equal, up to a scaling factor, to the found contour line. For any configuration of the triple lens there are six saddle points of the Jacobian. Hence, we obtain six values of $\det J'$ that tell us how to re-scale the lens positions to obtain parameters of critical-curve mergers.

As an example we present a triple lens with equal masses and arbitrary lens positions. The system is parametrized by the triangle circumference o and three lengths of sides as fractions of the circumference a, b, c, constrained by $a+b+c = 1$. Taking advantage of the symmetry of this problem we draw $o = \text{const}$ slices of the parameter space as ternary plots. The $o = 4.8$ slice is shown for illustration in Fig. 3. Here the parameter space is divided into nineteen regions, due to symmetry representing only six distinct types of regions, labelled in the Figures A through F.

Examples of critical curves and caustics corresponding to the six regions are presented in Fig. 4. There are altogether five different critical-curve topologies in this slice of the parameter space, with regions B and C having the same topology. The topologies in A and B / C do not occur in the two-parameter equilateral-triangle model described earlier. D has the same critical-curve topology as A in Fig. 2, their caustics have the same total number of cusps but the latter has four more intersections. The critical-curve topology and number of caustic cusps are the same for the following pairs of examples: E from Fig. 4 and D from Fig. 2; F from Fig. 4 and B from Fig. 2. Note that the example F in Fig. 4 has the parameters of an equilateral triangle; its parameters lie in B of Fig. 1.

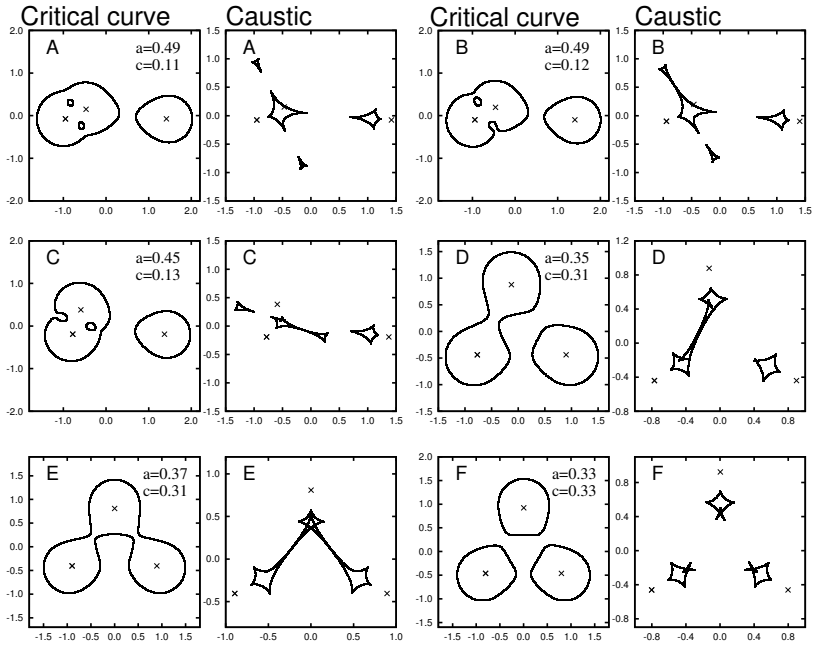

Figure 4. Critical curves and caustics of a triple lens with equal masses and circumference $o = 4.8$. First and third column: critical curves; second and fourth column: caustics; crosses: lens positions. Letters labelling the panels correspond to regions in Fig. 3.

5 CONCLUSION

The topological analysis of critical curves and caustics of binary lenses provides a priceless theoretical background for analysing observed microlensing light curves. We have shown that it is possible to find algebraic conditions for critical-curve merger for special two-parameter models of triple lenses. We have found a numerical method for obtaining merger parameters for a general multiple lens, by identifying the contour lines of the Jacobian passing through its saddle points with the critical curves of re-scaled lens configurations.

The number of possible critical-curve topologies in the full parameter space of a triple lens still remains unclear. For a more instructive insight into all possible light curves of triple-lens microlensing we also need to refine the analysis to cover other caustic transformations. In particular, the number of caustic cusps can change even without mergers. For a complete caustic-topology analysis, also caustic intersections should be taken into account.

ACKNOWLEDGEMENTS

This research project was supported by the Czech Ministry of Education project MSM00216-20860, by Czech Science Foundation grant GACR P209/10/1318 and by the projects SVV 263301 and GAUK 428011 of the Charles University in Prague.

REFERENCES

Chung, S.-J. and Park, B.-G. (2010), Properties of microlensing central perturbations by planets in binary stellar systems under the strong finite-source effect, *The Astrophys. J.*, **713**, p. 865.

Daněk, K. (2010), *Gravitational microlensing by a few-body system*, Charles University in Prague, Prague, master's thesis.

Erdl, H. and Schneider, P. (1993), Classification of the multiple deflection two point-mass gravitational lens models and application of catastrophe theory in lensing, *Astronomy and Astrophysics*, **268**, p. 453.

Gaudi, B. S. et al. (2008), Discovery of a Jupiter/Saturn analog with gravitational microlensing, *Science*, **319**, p. 927.

Han, C. (2008), Microlensing Detections of Moons of Exoplanets, *The Astrophys. J.*, **684**, p. 684.

Lee, D.-W. et al. (2008), Microlensing detection of planets in binary stellar systems, *The Astrophys. J.*, **672**, p. 623.

Liebig, C. and Wambsganss, J. (2010), Detectability of extrasolar moons as gravitational microlenses, *Astronomy and Astrophysics*, **520**, p. A68.

Refsdal, S. (1964), The gravitational lens effect, *Monthly Notices Roy. Astronom. Soc.*, **128**, p. 295.

Schneider, P. and Weiss, A. (1986), The two-point-mass lens: detailed investigation of a special asymmetric gravitational lens, *Astronomy and Astrophysics*, **164**, p. 237.

Witt, H. J. (1990), Investigation of high amplification events in light curves of gravitationally lensed quasars, *Astronomy and Astrophysics*, **236**, p. 311.